IJRAME
ISSN (ONLINE): 2321-3051

INTERNATIONAL JOURNAL OF RESEARCH IN AERONAUTICAL AND MECHANICAL ENGINEERING

STUDY OF THE TURBULENT NATURAL CONVECTION INSIDE A DIFFERENTIALLY HEATED SQUARE CAVITY

Tcheukam-Toko D.[*1], Tientcheu-Nsiéwé M.[2], Mouangue R.[3], Djanna-Koffi F.[4], Kuitche A.[5]
[1, 3] Department of Energetic Engineering, University Institute of Technology, Ngaoundere
P.O. Box 455 Ngaoundere, Cameroon
[2, 5] Department of Energetic Engineering, University Institute of Technology, Douala
P.O. Box 8698 Douala, Cameroon
[4] Department of Electric, Energy and Automatism Engineering, ENSAI of Ngaoundéré,
P.O. Box 455Ngaoundere, Cameroon
* Corresponding author. Email: tcheukam_toko@yahoo.fr
Tel: +237 97 66 47 37 / +237 77 76 08 61; Fax: +237 22 25-27-51

Abstract
The turbulent natural convection inside a differentially heated square cavity has been studied numerically in this paper. Special attention has been paid for the wall effect on the convection. The turbulent model has been applied a standard κ-ε two equations model and the two-dimensional Reynolds Averaged Navier–Stokes (RANS) equations are discredited with the second order upwind scheme. The SIMPLE algorithm, which is developed using control volumes, is adopted as the numerical procedure. Calculations were performed for a wide variation of Rayleigh number corresponding to different flow. The results reveal that with increasing Rayleigh number, distributions of temperature and velocity show higher values at the wall region of the cavity. Comparison of numerical results with the experimental data available in the literature is satisfactory.

Key words: Turbulent natural convection, differentially heated cavity, thermal field, dynamic field, boundary layer, CFD.

1. Introduction

The steady study of a fluid particle in a gravity field is a very important phenomenon. The steady state is possible if the volumes forces as the weight must be compensated with the pressure gradients, which are very depended to mass conservation condition. To destroy this steady, we need for example to modify locally the density of fluid, by the dissolution of a salt or by causing its thermal dilatation. The movement generated by this density variation is called « natural convection ». It's at the beginning of 20th century that the concept of convection was defined by Bénard in 1901 and then, Rayleigh in 1916. The temperature gradient control inside a heated cavity or an air conditioning cavity is a complex processes. This could generate a great heat loss, and to characterize the thermal ambiance of a cavity will allow a reducing of the energetic loss and an opening new way in the construction industry development. In this domain, the principal use of energy concerns the comfort, such as heating and air conditioning.

In order to increase the efficiency of these energetic systems, it's very important to known the convections flows generated by the heating or the air conditioning. The heat transfers inside a cavity are generated by the natural convection and radiation. Many works have been carried out such as Batchelor [1], Le Quéré [2], and Aklouche S. and *al* [3], who have studied the different flows regimes for the lower Rayleigh numbers ($Ra < 10^5$), and the transition to the turbulence inside the differentially heated cavity. Ndame [4], Salat [5], Mergui [6], Benkhelifa A. and *al* [7], and Djanna-Koffi [8], have done a quantitativly and qualitativly analysis for the higher Rayleigh numbers ($Ra = 10^9$ à 10^{12}). Then, Wang H. and *al* [9], Ibrahim A. [10], have shown the influence of surface radiations on the thermal stratification in the middle and inside the boundary layer near the wall of the cavity. For the best understanding of surfaces radiation on the natural convection, a numerical simulation of the turbulent natural convection inside a square cavity filled by the air, have been carried out in this work. This physical domain is the same with experimental woks of Wang and *al* [9]. To lead well this study, we are going to explain the mathematical formulation and the computation procedure used to calculate the thermal and dynamic fields, with or without taking in account the surface radiations, for a wide variation of Rayleigh numbers. The results will be compared with the experimental results of Wang and *al* [9].

2. MATHEMATICAL FORMULATION AND COMPUTATION PROCEDURE

2.1. Assumption of calculation domain

We have based our study on the experimental work of Wang and *al* [9], carried out inside a square cavity of 0.335 x 0.335 m^2 filled by the transparent air, treated as grey gas, and represented by the figure 1 bellow. The cavity walls are the adiabatic surfaces and the vertical ones are isothermals and are maintained at constant temperature (T_c for the hot wall and T_f for the cold wall).

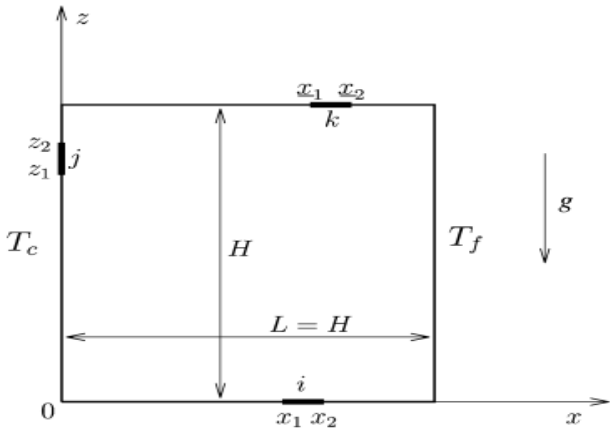

Figure 1: Physical domain of the square cavity:$T_0 = (T_c + T_f)/2$ and $T = T_c - T_f$.

2.2 Governing equations

The heated flow through the cavity is described by a set of non-linear partial differential equations expressing the physical laws of conservation between the velocity, pressure and temperature at each point of the flow: the Navier-Stokes and the equation of energy conservation. To these equations, we add the equation of turbulent kinetic energy and that of its dissipation rate like proposed by Launder and Spalding [11]. Solving these equations will reveal features such as thermal and dynamic fields. By adopting the simplifying assumptions above and for a steady flow, all governing equations and turbulence equation model are expressed in terms of a single general differential equation (1), by combining the convective and diffusive terms together. The details of this analysis can be found in Patankar [12].

$$\frac{\partial}{\partial x}(\rho\langle u\rangle\psi)+\frac{\partial}{\partial z}(\rho\langle v\rangle\psi)=\frac{\partial}{\partial x}\left(\Gamma_\psi\frac{\partial\psi}{\partial x}\right)+\frac{\partial}{\partial z}\left(\Gamma_\psi\frac{\partial\psi}{\partial z}\right)+S_\psi \qquad (1)$$

Where ψ is the dependent variable (velocity, turbulent kinetic energy, temperature...), Γ_ψ is the diffusion coefficient of ψ and S_ψ represents the source term of the magnitude considered. These variables are given in Table 1 bellow. In this table, μ_{eff} represents the effective dynamic viscosity; S_u and S_v are respectively the axial and vertical source terms. G_k is the production term reflecting the transfer of the kinetic energy of the mean flow to the turbulent flow through the interaction between fluctuations and mean velocity gradients, and G_b represents the effects of buoyancy on turbulent kinetic energy. The equations (2), (3), (4), (5) and (6), represent their formulas.

Table 1: Expressions for ψ, Γ_ψ, and S_ψ

Governing Equations	ψ	Γ_ψ	S_ψ
Continuity	1	0	0
Vertical momentum	$\langle v\rangle$	μ_{eff}	$-\frac{\partial\langle p\rangle}{\partial z}+\frac{\partial}{\partial z}\left(\nu_{eff}\frac{\partial\langle v\rangle}{\partial z}\right)+S_v$
Axial momentum	$\langle u\rangle$	μ_{eff}	$-\frac{\partial\langle p\rangle}{\partial x}+\frac{\partial}{\partial z}\left(\nu_{eff}\frac{\partial\langle u\rangle}{\partial z}\right)+S_u$
Energy	$\langle\theta\rangle$	$P_{rt}(\mu_{eff}/\sigma_t)+1$	0
Turbulent kinetic energy	K	$\mu_l+(\mu_t/\sigma_k)$	$G_k+G_b-\rho\varepsilon$
Dissipation rate	E	$\mu_l+(\mu_t/\sigma_\varepsilon)$	$C_{1\varepsilon}\frac{\varepsilon}{\kappa}(G_\kappa+C_{3\varepsilon}G_b)-C_{\varepsilon 2}\frac{\varepsilon^2}{\kappa}$

$$\mu_{eff}=\mu+\mu_t=\mu+c_\mu\frac{\kappa^2}{\varepsilon} \qquad (2)$$

$$S_v=\frac{\partial}{\partial z}\left(\nu_{eff}\frac{\partial\langle v\rangle}{\partial z}\right)+\frac{\partial}{\partial x}\left(\nu_{eff}\frac{\partial\langle v\rangle}{\partial x}\right) \qquad (3)$$

$$S_u=\frac{\partial}{\partial z}\left(\nu_{eff}\frac{\partial\langle u\rangle}{\partial z}\right)+\frac{\partial}{\partial x}\left(\nu_{eff}\frac{\partial\langle u\rangle}{\partial x}\right) \qquad (4)$$

$$G_\kappa=\mu_t\left[\left\{2\left(\frac{\partial\langle v\rangle}{\partial z}\right)^2+\left(\frac{\partial\langle u\rangle}{\partial x}\right)^2\right\}+\left(\frac{\partial\langle v\rangle}{\partial z}+\frac{\partial\langle u\rangle}{\partial x}\right)^2\right] \qquad (5)$$

$$G_b=\beta g\frac{\mu_t}{P_{rt}}\left[\frac{\partial}{\partial z}\langle T\rangle\right] \qquad (6)$$

Where, C_μ, $C_{1\varepsilon}$ and $C_{2\varepsilon}$ are empirical constants; σ_ε and σ_k are respectively the turbulent Prandtl numbers force and ε; P_{rt} is the turbulent Prandtl number those value are between 0.9 and 1 in the literature. The values of these constants proposed by Jones and Launder [11], are in table 2 bellow.

Table2: Empirical constants proposed by Jones and Launder [11].

C_μ	$C_{1\varepsilon}$	$C_{2\varepsilon}$	σ_k	σ_ε
0.09	1.44	1.2	1.0	1.3

2.3 Computation procedure

The transition from physical domain to the numerical domain begins with the generating mesh geometry by a preprocessor. Then import this into a computational code for the iterative solution of equations to determine the values of variables on each node of the mesh. The segregated solution method was chosen for the resolution of turbulence model and governing equations. Governing equations were discredited with the control volume technique. For the convective and the diffusive terms, a second order upwind method was used while the SIMPLE (Semi Implicit Method for Pressure Linked Equations), procedure was introduced for the velocity-pressure coupling (Patankar [12], Tcheukam-Toko D. and *al*. [13]). The convergence of the numerical calculation is checked by examining the evolution of relative residuals in each governing equation for a convergence criterion of 0.001%. The stability of the iterative process was carried out by relaxation coefficients associated with the velocity, pressure, temperature, κ, ε and μ_t. The Standard Wall-Functions were used to take into account the effects of friction near the wall. Three mesh distributions have been tested to ensure that the calculated results are grid independent.

3. RESULTS AND DISCUSSION

3.1 Generating mesh geometry

The figure 2 bellows represents the computational domain meshed with the code GAMBIT. The grid distribution is a set of quadrilateral cells (uniformly structured mesh). The calculations will used the software FLUENT.

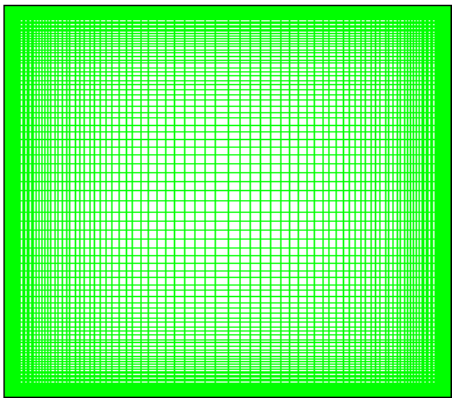

Figure 2: Grid configuration

The mesh is very uniformly fine near the walls where the velocity and temperature gradients are large. The grid distribution impacts the computation time and the number of iterations required for the solution converge. The

choice of the mesh size of 112,225 cells is a good compromise and the results that will be presented later are those of this mesh size. The no-dimension variables are:

$$X+ = X/H \quad (7)$$

$$Z+ = Y/H \quad (8)$$

$$U+_x = U/U_{max} \quad (9)$$

$$T^+ = T/T_{max} \quad (9)$$

3.2 Thermal field

The figure 3 bellow represents the thermal field for different Rayleigh numbers: It shows that the differentially heated square cavity have a principal flow with the thermals boundaries layers along the actives walls (one is ascendant along the hot wall and the order is descendant along the cold wall), and also the walls jets along the floor and the ceiling connecting the two boundaries layers. We observed also the presence of secondary recirculation zones above of floor wall jet and bellow of ceiling. Qualitatively, the thermal field is not varied, because the turbulent flow regime has not change, while quantitatively, the thermal stratification at the middle of the cavity is varying.

a) Ra = 3.14 10^7

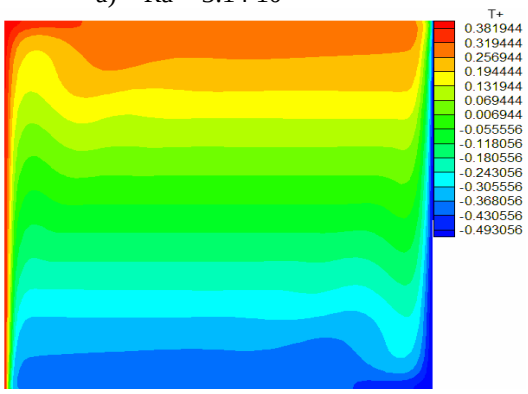

b): Ra = 3.94 10^7

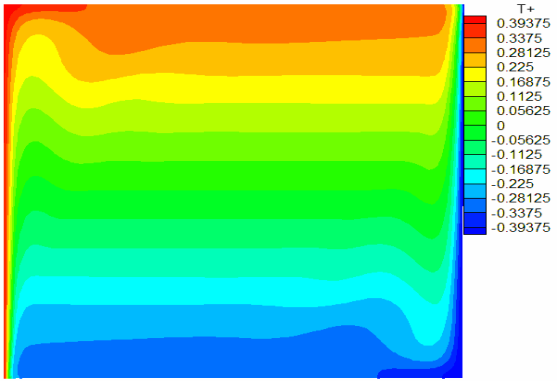

c): Ra = 1.04 10^7

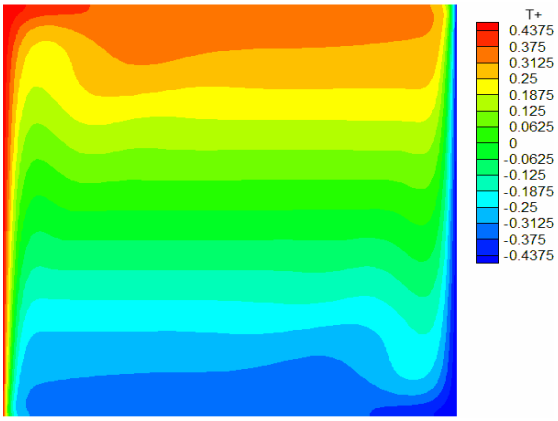

Ra = 2.79 10^7

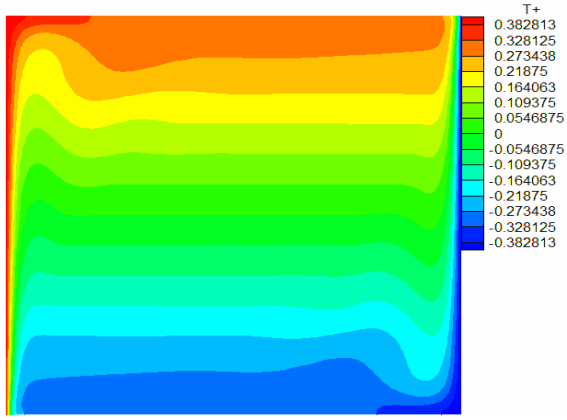

Figure3: Thermal field for different Rayleigh numbers

The figure 4 bellow represents the temperature profiles near the higher wall, lower wall and, at the middle of the cavity. We observed that the thermal boundary layer is coming closer the higher wall when the Rayleigh is decreasing and contrary to the lower wall.

a) b)

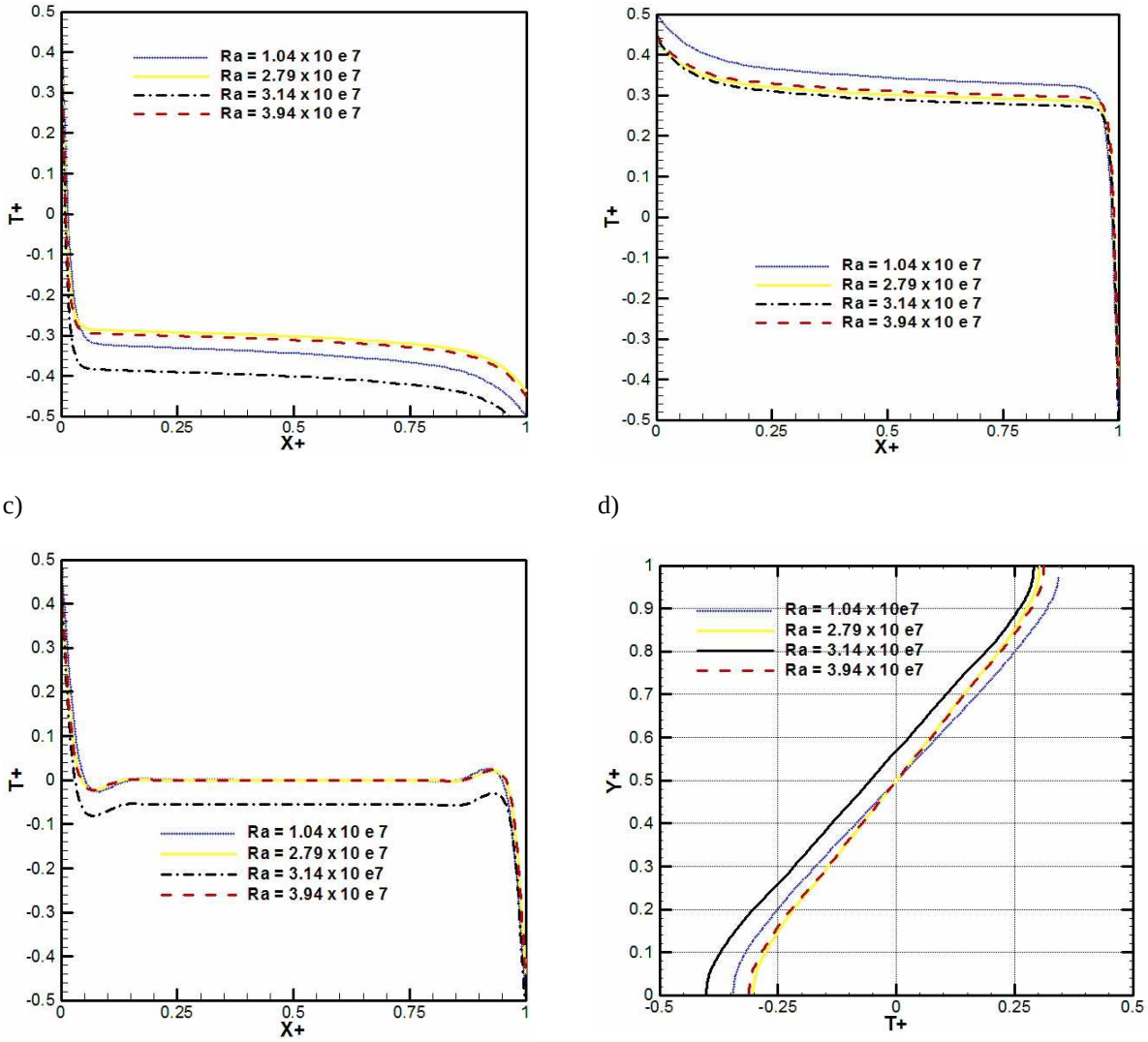

c) d)

Figure 4: *Temperature profiles for different Rayleigh numbers. a): near the lower wall, b): near the higher wall, c) and d): at the middle of the cavity*

The temperature profiles at the middle of cavity (medium length and medium height), is linear and becoming symmetry compared with the center. Near the floor and the ceiling, these profiles are not linear because of wall jet and probably, of surface radiation which is not negligible.

3.3 Thermal field with surface radiation

The figure 5 bellow represents the thermal field for different Rayleigh numbers, in the cases where the walls are not emissive ($\varepsilon = 0$), and when they have a low emissivity ($\varepsilon = 0.20$). The volume radiation shows two new recirculation zones in the corners (above at left and bellow at right), to the detriment of hydraulics jumps observed in the case of pure convection. The wall radiation increases the diminution of recirculation zones near the actives

walls and modified the flow structure, with the appearance of new recirculation zones in upstream from the hot and cold boundaries layers.

The figure 6 represents the temperature profiles for different emissivity. We observed a distortion of the recirculation zone near the actives walls, with a strong tendency to supply the opposite boundary layer.

a) Ra = 1.04 10^7 b) Ra = 2.79 10^7

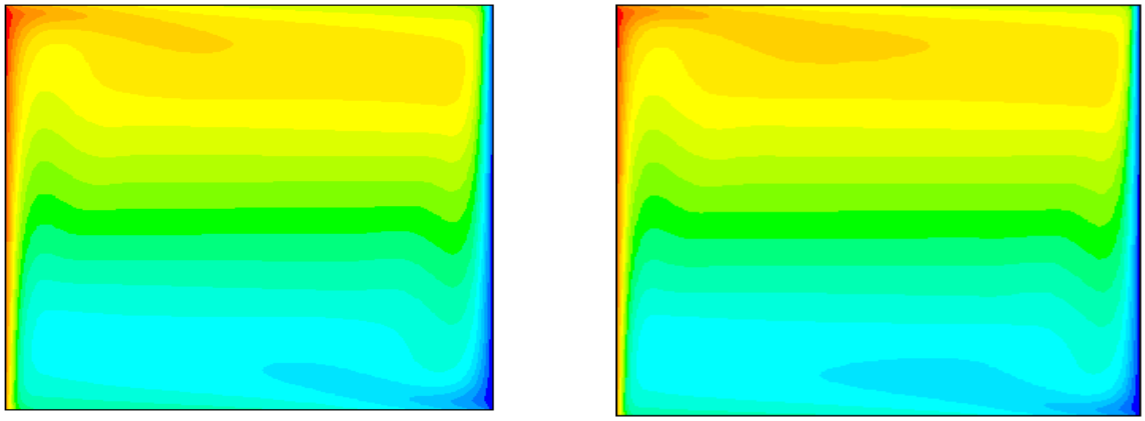

***Figure 5**: Thermal field with surface radiation*

a) b)

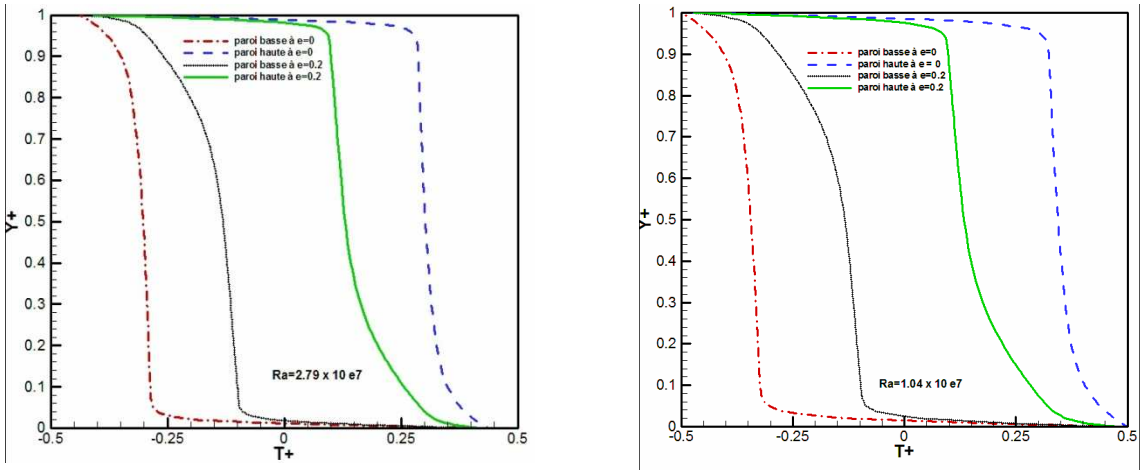

Figure 6: Temperature profiles for different emissivity. a): near the floor; b): near the ceiling

The figure 7 represents the temperature profiles at the middle of the cavity. In the case R_a = 1.04 x10^7, the stratification parameter is 0.33; in the case without radiation of passive walls, and 0.40; in the case with radiation (ε = 0.20), its means that a diminution of 32%.

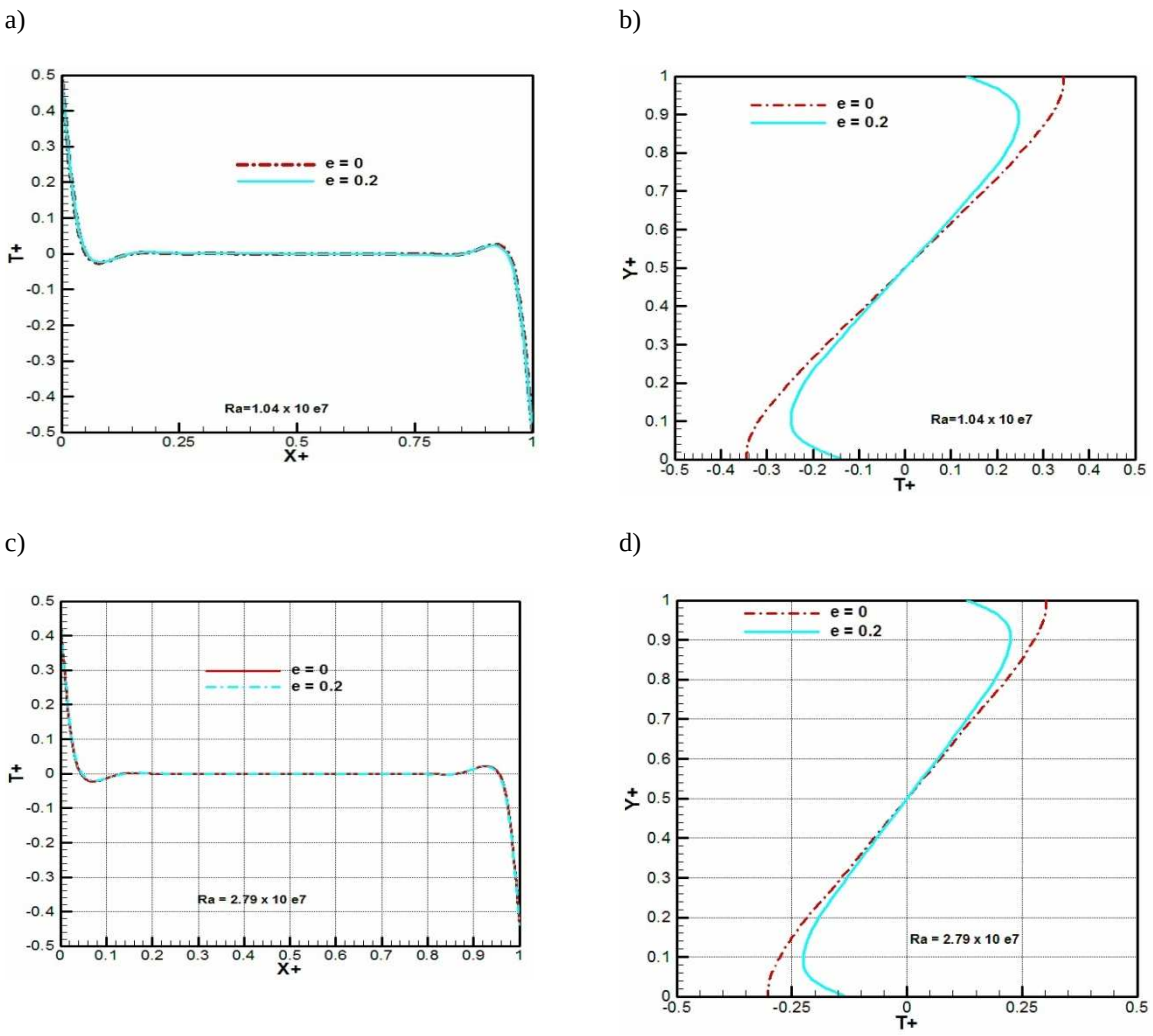

Figure 7: Temperature profiles at the middle of cavity for different emissivity. a) and b): at the medium height; c) and d): at the medium length.

We observed that the volume radiation decreases also the thermal stratification at the middle of cavity, but remains low compared with the observation in the case of surface radiation.

3.4 Dynamic field

The figure 8 bellow represents the dynamic field for different Rayleigh numbers. We observed that the flow is modifying quantitatively and qualitatively. When the Rayleigh number increase, the dynamic boundary layer take a long time to take off. The great values of velocities are located in the boundary layer over the vertical wall, but remain low since the maximum velocity is less than 14% of the velocity reference.

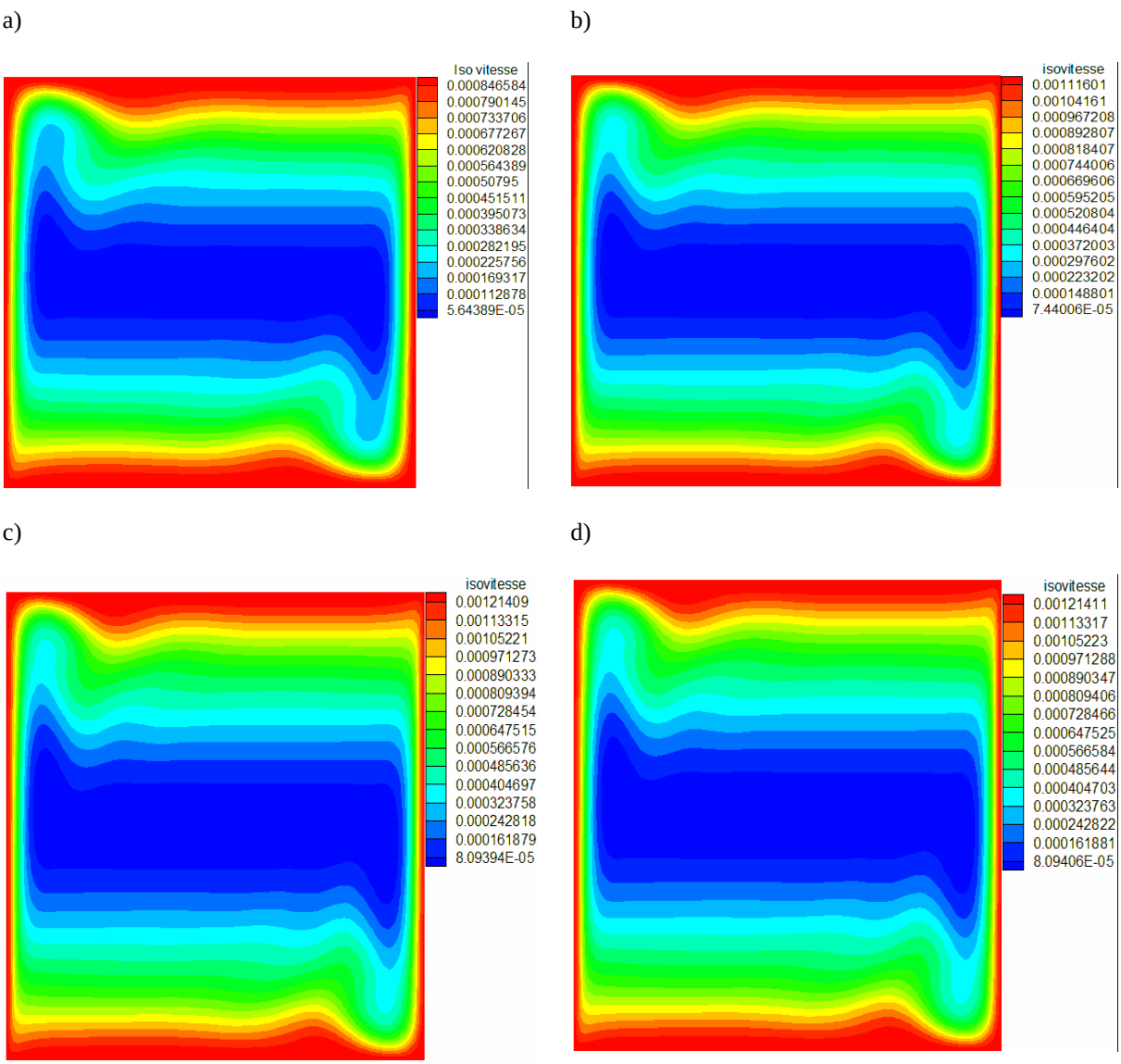

Figure 8: Dynamic field for different Rayleigh numbers

The figure 9 bellow represents the vertical velocity profiles in the hot and cold boundary layer. We observed that the maximum velocity of wall jet near the ceiling, at the medium length, is the same for all the Rayleigh number (the relative scale is less than 6%). This type of flow is characterized by the presence of an ascendant boundary layer along the hot wall and a descendant boundary layer along the cold wall, connected by a wall jet on the floor and the ceiling.

a) b)

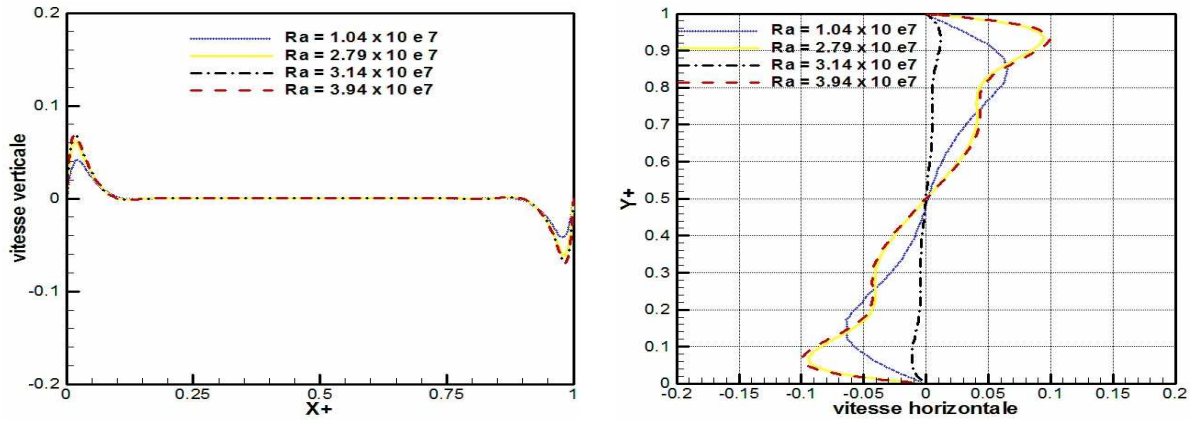

Figure 9*: Vertical (a), and horizontal (b), velocities profiles at the medium length (b) and medium height (a).*

3.5 Dynamic field with surface radiation

The figure 10 bellow represents the dynamic field taking in account the surface radiations, and the figure 11 represents the vertical and horizontal velocities profiles in the heart of the cavity. We observed that the wall radiation increases the weakening of recirculation zones near the actives walls and modify the flow structure, with the appearance of new recirculation zones in upstream from the hot and cold boundaries layers.

a) b)

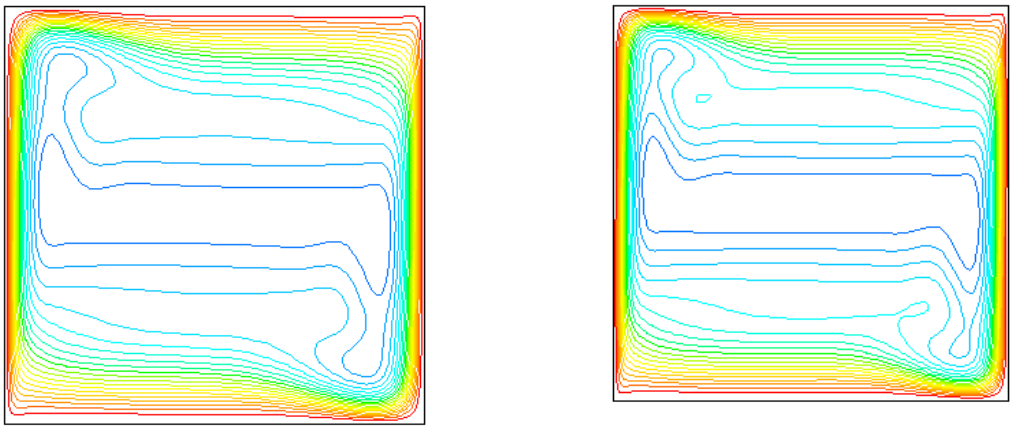

Figure 10: Dynamic field with surface radiation. a): Ra = 1.04 x 10^7, b): Ra= 2.79 x10^7

The figure 11 shows that at medium length, the radiation inverts the flow symmetry. On the contrary, at medium height, there is no change on the velocity curve. The wall radiations modify the flow structure promoting the formation of secondary flows near the horizontal wall. They also decrease the thermal stratification at the heart of cavity and modify the thermal transfer near the actives walls.

3.6 Comparisons with the experimental results

We have compared our results to the experimental results of Wang H. et *al* [9], carried out on the natural convection near the grey walls inside a differentially heated square cavity, filled of air (Pr = 0.71). The thermal field represented at the figure 12 bellow, show the same tendency with those of Wang H. and *al* [9]. The flow is also symmetry compared with the center.

a) b)

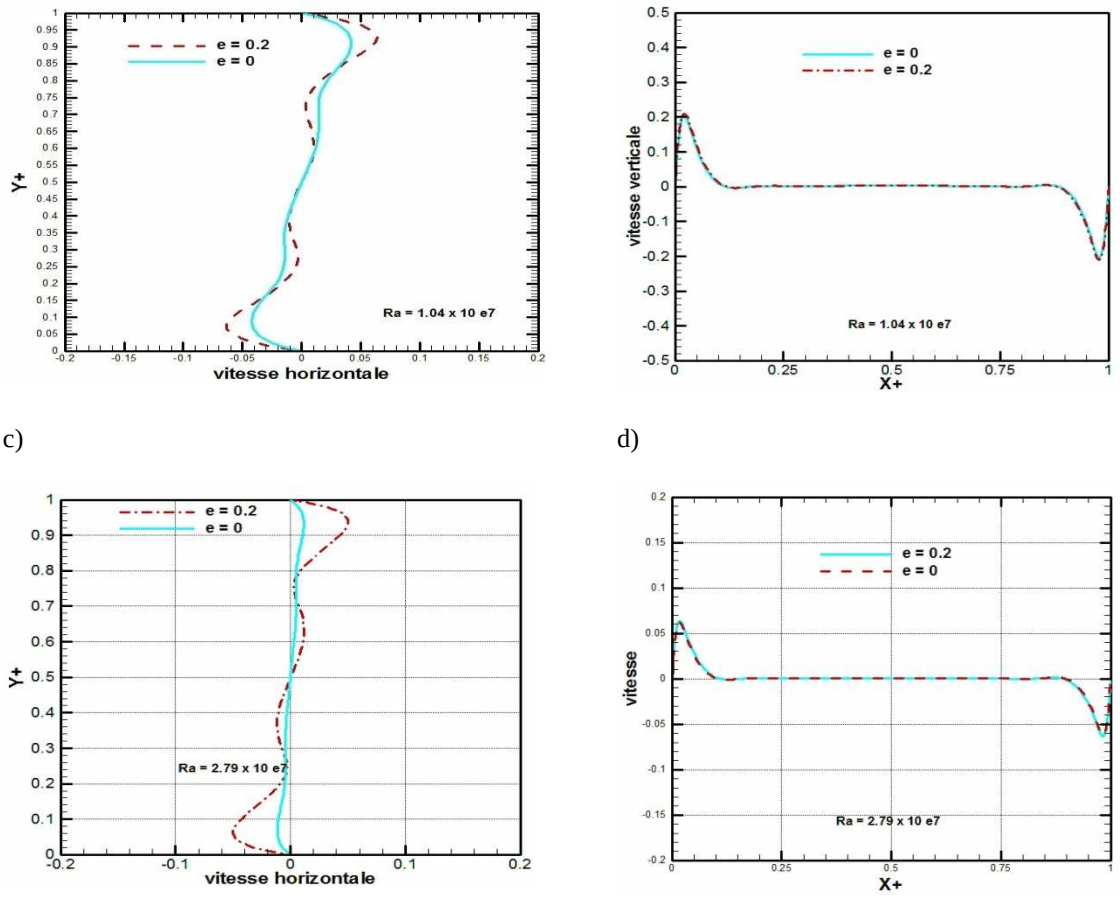

c) d)

Figure 11:*Vertical and horizontal velocities profiles in the heart of cavity for Ra = 10^7*

a) b)

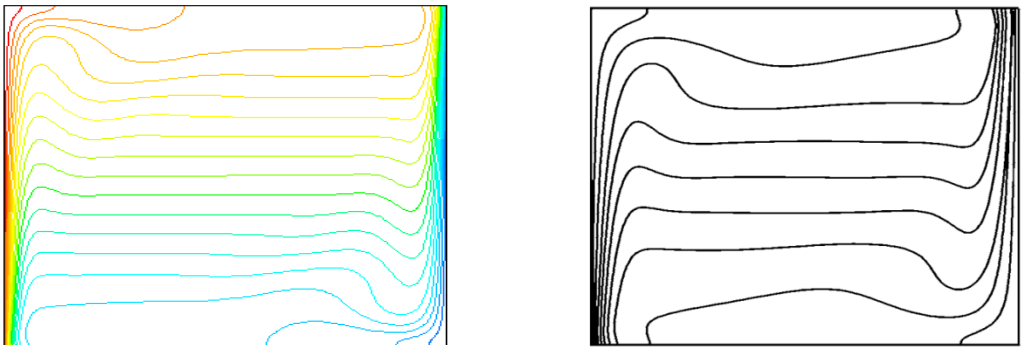

Figure 12*: Thermal field: a): This study, b): experimental results of Wang H and al[9].*

The figure 13 bellow represents the temperature profiles for the ceiling and the floor. We observed that the ceiling loss the heat (net heat flux positive), while the floor receive the heat (net heat flux negative). Wang H. et *al* [9] obtain the same result and at the medium length and medium height, the two results (numerical and experimental), shows a good concordance.

a) b)

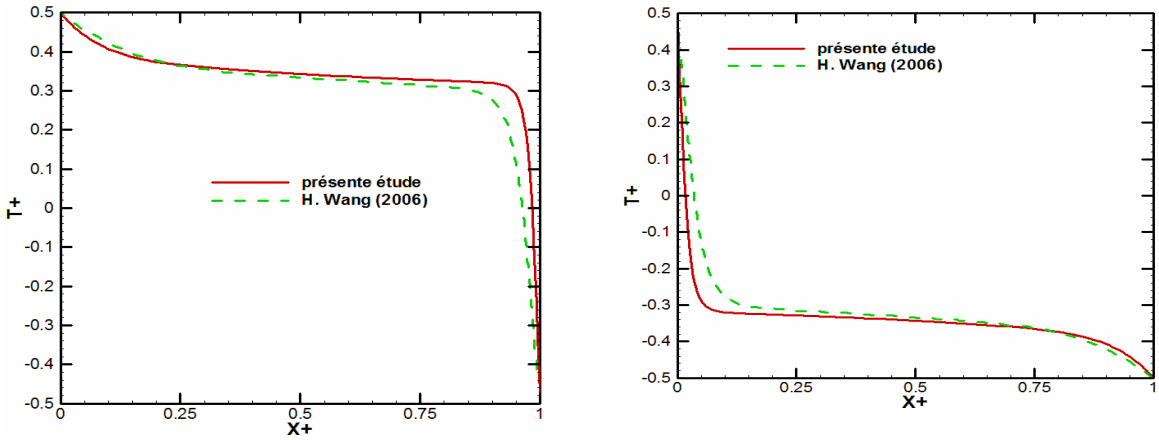

Figure 13: Temperature profiles for Ra = 10^6. a): on the ceiling; b): on the floor.

The figure 14 bellow represents the comparison of dynamics fields. It shows qualitatively the same contour. The velocities profiles at medium length represented in figure 15 are similar and confirm this satisfactory.

a) b)

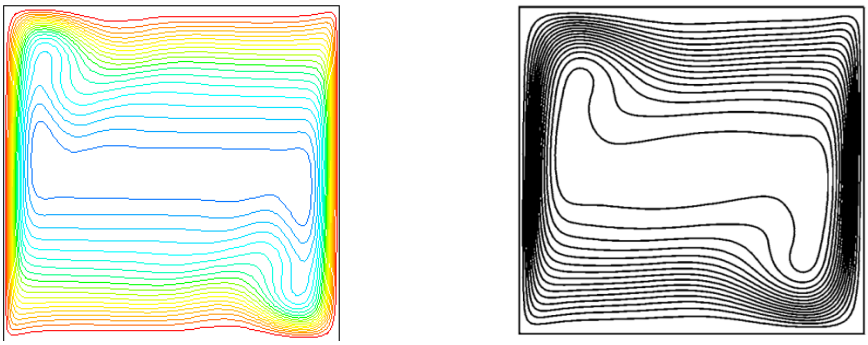

Figure14: Dynamic field. a): this study, b): Wang H. et al [9]

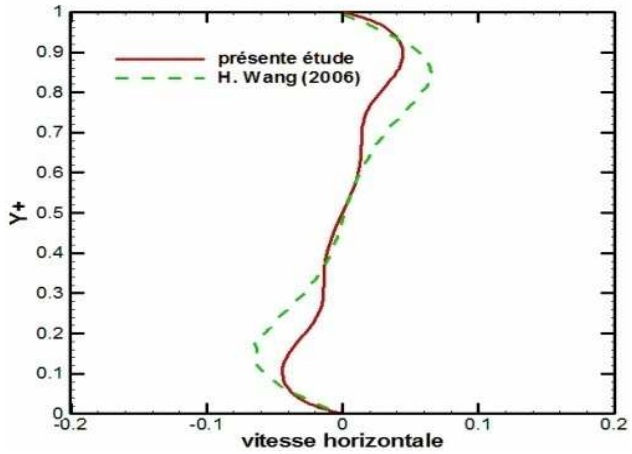

***Figure 15**: Velocity profile at the medium length of the cavity for Ra = 10^6*

4. CONCLUSIONS

These results reveal the influence of surface radiation on the thermal and dynamic fields. An ascendant boundary layer and a descendant boundary layer should be observed respectively along the hot and cold wall. The walls jets along the floor and the ceiling are connecting the two boundaries layers. The different comparisons makes between the numerical and experimental profiles are satisfactory. In perspectives, it would be interesting to associate the heated air jets to this present study, in order to analyze their influence on the stability of thermal and dynamic fields.

BIBLIOGRAPHIE

[1] Batchelor G. K. Heat transfer by free convection across a closed cavity between vertical boundaries at different temperatures. Quaterly of Applied Mathematics, 12: 209-233, 1954.

[2] Le Quéré P. Etude de la transition à l'instationnarité des écoulements de convection naturelle en cavité verticale différentiellement chauffée par méthodes spectrales Chebyshev, Thèse de doctorat ès Sciences, Université de Poitiers, France, 1987.

[3] Aklouche S., Zeghmati B., Bouhadef K., Daguenet M. Etude numèrique de la convection naturelle instationnaire bidimensionnelle dans une enciente fermée. Identification des routes vers le chaos. *Journée International de Thermique.* Pp. 65-68, Maroc, 2005.

[4] Ndame A., Etude expérimentale de la convection naturelle en cavité : De l'état stationnaire au chaos. Thèse de Doctorat, Université de Poitiers, France, 1992.
[5] Salat J., Xin S., Joubert P., Sergent A., Penot F., Le Quéré P. Experimental and numerical investigation of turbulent natural convection in a large air-filled cavity. International Journal of Heat and Fluid Flow, Vol. 25, pp. 824-832, 2004.
[6] Mergui S. Caractérisation expérimentale des écoulements d'air de convection naturelle et mixte dans une cavité fermée. Thèse de Doctorat. Université de Poitiers, France, 1993.
[7] Benkhelifa A., Fuentes C., Tuhault J. L., Penot F. Convection naturelle à grand nombre de Rayleigh dans une couche horizontale de fluide, approche expérimentale. Journées Internationales de Thermiques. Pp. 1-5, Albi-France, 2007.
[8] Djanna-Koffi F. L., Convection naturelle turbulente en cavité différentiellement chauffée à grands nombres de Rayleigh : caratérisation expérimentale des écoulements et des transferts thermiques, étude numérique du couplage convection-rayonnement. Thése de Doctorat, Ecole Nationale Superieure de Mecanique et D'aerotechnique Poitier, France, 2011.
[9] Wang H., Xin S., Le Quéré P., Étude expérimentale du couplage de la convection naturelle avec le rayonnement de surfaces en cavité carrée remplie d'air. Comptes Rendus de Mécanique, pp. 48-57, 2005.
[10] Ibrahim A., Couplage de la convection naturelle et du rayonnement dans des mélanges gazeux absorbants-émettant, Thèse de Doctorat de l'Université de Poitiers, France. 2010.
[11] Launder B. E., and Spalding D. The numerical computation of turbulent flows, Computational Methods. App. Mech. Engineering, Vol. 3, pp. 269-289.1974.
[12] Patankar S.V., Numerical heat transfer and fluid flow, McGraw Hill, New-York, 1980
[13] Tcheukam-Toko D., Tagne-Kaptue B. S., Kuitche A., Mouangue R., and Paranthoën P.,. Study of turbulent flow downstream from a linear source of heat placed inside the cylinder wake. International Journal of Mechanical Engineering and Technology (IJMET), Vol. 4, issue 1: pp. 15-24, 2013.
[14] Rouger N., Sensibilité de la convection naturelle en cavité différentiellement chauffée à des variations de paramètres géométriques, thermiques et massiques. Thése de Doctorat, École Doctorale : Sciences pour l'Ingénieur et Aérotechnique Secteur de recherche : Énergétique, Thermique, Combustion, Poitier, France. 2009.